Available online at www.sciencedirect.com

ScienceDirect

Ceramics International 40 (2014) 745–752

CERAMICS INTERNATIONAL

www.elsevier.com/locate/ceramint

Fabrication of ceramic coatings from polysilazane/aluminum: Effect of aluminum content on chemical composition, microstructure, and mechanical properties

Fengyan Xiao[a,b], Zongbo Zhang[a], Fan Zeng[a], Yongming Luo[a,*], Caihong Xu[a,*]

[a]Institute of Chemistry, Chinese Academy of Sciences, Beijing 100190, China
[b]Graduate University of Chinese Academy of Sciences, Beijing 100049, China

Received 23 May 2013; received in revised form 18 June 2013; accepted 18 June 2013
Available online 26 June 2013

Abstract

Ceramic coatings with a thickness range of 1.5–5.5 μm were successfully prepared with polysilazane (PSN1) as a precursor and aluminum (Al) powder as an active filler. The effect of Al content on chemical composition, microstructure, and mechanical properties of the coatings was investigated. Chemical composition analysis revealed that Al powder was completely converted into Al_2OC and AlN phases during the ceramization process, accompanied by volume expansion. Ceramic coatings derived from less Al powder containing PSN1/Al showed more compacted surface morphology and continuous microstructure. The surface hardness and elastic modulus of ceramic coatings decreased with the increase of the volume fraction of Al from 10% to 40% (Al/PSN1, v/v). The maximum surface hardness and elastic modulus of coatings were 6.38 GPa and 107.66 GPa, respectively.

Keywords: C. Mechanical property; Polysilazane; Aluminum powder; Coatings; Microstructure

1. Introduction

In the past two decades, ceramics and ceramic composites have been successfully and conveniently fabricated by the well-known polymer-derived ceramics (PDCs) route, which has drawn intensive attention due to several advantages over traditional ceramic processing methods, including lower fabrication temperature, compositional homogeneity in the final products, the ability to use polymer-process techniques for processing complex-shaped components and the capability of property tailoring via composition design or thermal treatment parameters adjusting [1–5]. The PDCs route has a great variety of potential applications in the fabrication of bulk ceramics [6,7], ceramic composites [8,9], fibers [10,11], joining material [12], porous materials [13–15], micro electro-mechanical systems [16,17], protective coatings [18–25], and other materials [26]. Among them, preparation of protective coatings from preceramic polymers has been one of the most promising areas.

However, the coatings obtained from PDCs route generally suffer from formation of cracks, unwanted porosity, or even delamination due to large shrinkage of the polymer during cross-linking and pyrolysis process [4,27,28]. How to prepare crack-free and dense ceramic coatings is still a great challenge for the PDCs method. Many researchers reported that the addition of suitable amount of passive or active inorganic filler to the precursor could alleviate these problems [3,28,29]. Passive fillers cannot react with the matrix, and simply dilute the preceramic polymer, thereby reducing the shrinkage of the component upon ceramization and eliminating the occurrence of macrodefects. By contrast, active fillers such as metallic or intermetallic compounds do not only dilute the preceramic polymer, but also react with gaseous byproducts, the heating atmosphere, or the ceramic residue, which brings about volume expansion available to compensate for the shrinkage and thus enables the fabrication of low-porosity and crack-free ceramic coatings.

*Corresponding authors. Tel./fax: +86 10 62554487.
E-mail addresses: luoym@iccas.ac.cn (Y. Luo), caihong@iccas.ac.cn (C. Xu).

0272-8842/$ - see front matter © 2013 Elsevier Ltd and Techna Group S.r.l. All rights reserved.
http://dx.doi.org/10.1016/j.ceramint.2013.06.064

Aluminum (Al) powder is commonly used as an active filler due to its high activity and high temperature resistance of formed products. Wang et al. [30] prepared high infrared emissivity coatings with good thermal stability using Al powder as an expansion agent and poly(hydridomethylsiloxane) (PHMS) as polymer precursor. The high infrared emissive property was attributed to the complete conversion of Al into Al_2O_3 and PHMS into SiO_2 at low temperature, as well as the high emissivity enhanced filler agent HW (mixture powders based on SiC). Yang et al. [31] demonstrated the fabrication of dense SiC coatings from the mixture of polycarbosilane and Al powder. However, to our knowledge, research about ceramic coatings based on polysilazane/Al has not been reported. Moreover, the effect of microstructure and composition of coatings derived from preceramic polymer/Al on mechanical properties was not investigated.

In this paper, crack-free ceramic coatings were successfully fabricated using polysilazane (PSN1) as a preceramic polymer and Al powder as an active filler. The influence of the volume of Al powder on the composition, microstructure, and mechanical properties of the coating was studied.

2. Experimental

2.1. Materials

The liquid polysilazane (PSN1, –[SiNH(CHåCH$_2$)]$_x$–[NHSiNH(CH$_3$)]$_y$–, Mn = 600–1000) was synthesized according to the reported method [32]. Al powder with a particle size of 3–5 μm was obtained from Beijing Dekedaojin Co. Ltd. (Beijing, China). Xylene was purchased from Beijing Chemical Works (Beijing, China) and distilled with calcium hydride prior to use. Dicumyl peroxide (DCP) was obtained from Sinopharm Chemical Reagent Co. Ltd. (Beijing, China) and purified by standard process. Flat stainless steel (AISI 304, thickness: 1 mm) was purchased from Guangdong Zhuyou Stainless Steel Co. Ltd. (Chaozhou, China). Before applying coatings, the stainless steel sheets with dimensions of $10 \times 10\ mm^2$ were washed with acetone, ethanol, and distilled water by ultrasonic treatment respectively, and then dried in nitrogen.

2.2. Preparation of coatings

A slurry dip process was used to prepare the coating. 10–40 vol% Al powder and 0.5 wt% DCP were added to the PSN1 and the mixture was diluted using xylene (solvent) to suit for the dip process. After stirring for 30 min, the slurry was then ball milled for 4 h. The detailed formulations of the slurry are listed in Table 1. The pretreated 304 stainless steel substrates were dip-coated with a hoisting apparatus at a withdrawal rate of 5 mm/s. The coated substrates were heated at 170 °C for 2 h in the oven to allow cross-linking. The cured coatings were pyrolyzed in the tubular furnace under nitrogen atmosphere. The samples were heated at 1 °C/min to 450 °C and held for 1 h, and then the coatings were performed up to 800 °C with heating rate of 5 °C/min and holding time of 1 h under flowing nitrogen, and then temperature decreased to the room temperature at the rate of 5 °C/min.

Table 1
The detailed formulations of the slurry.

Sample	Filler	Solvent	V(Al)/V (PSN1) (%)	V(PSN1+Al)/V(xylene)	Viscosity (C_p)
PSN1/Al-1	Al	Xylene	10	2:5	1.04
PSN1/Al-2	Al	Xylene	20	2:5	2.07
PSN1/Al-3	Al	Xylene	30	2:5	3.11
PSN1/Al-4	Al	Xylene	40	2:5	5.18

The solvent of the residue slurry was firstly removed by distillation, then cured and pyrolyzed in the same procedure with the heat treatment of the coatings. The obtained powders were used for the relative characterization.

2.3. Characterization methods

Thermal gravimetric analyses (TGA) were carried out on a SII EXSTAR TG/DTA6300 instrument in nitrogen atmosphere at a heating rate of 10 °C/min.

The viscosity was measured on a Brookfield HADV-II viscometer at 25 °C.

Fourier transform infrared (FT-IR) spectra were obtained from a Bruker Tensor-27 FTIR spectrometer in the wavenumber range of 4000–400 cm^{-1}.

X-ray diffraction (XRD) measurements were carried out on a Rigaku D/M4X 2500 diffractometer with Cu-Kα radiation.

X-ray photoelectron spectroscopy (XPS) data were obtained with an ESCALab220i-XL electron spectrometer from VG Scientific (East Grinstead, UK) using 300 W Al-Kα radiations.

The surface and cross section morphologies of the coatings were observed using Hitachi S-4800 scanning electron microscopy (SEM).

The hardness and Young's modulus of the coating were measured by MTS XP Nano-indentation with a Berkovich diamond indenter. The measurements were performed five times with a contact depth ranging from 50 to 300 nm.

3. Results and discussion

3.1. Ceramic yields of cross-linked PSN1 and PSN1/Al

Several criteria need to be considered when selecting a preceramic polymer for the specific application. The first is that the polymer must have a high ceramic yield upon pyrolysis. High ceramic yield polymers are easier to densify and have lower tendency to form cracks and unwanted pores when applied in coatings [4]. Therefore, the ceramic yields of cross-linked PSN1 with different content of Al expansion agent were characterized by TGA measurement. The results of TGA analyses in nitrogen are given in Fig. 1. It can be seen that the ceramic yield of the cross-linked samples was clearly enhanced with increasing of Al content. The ceramic yield of the cross-linked PSN1 without Al was only 72.9% at 800 °C, whereas the ceramic yields of the cross-linked PSN1 with 10–40 vol% Al powder ware up to 77.8%,

84.8%, 89.4%, and 90.7%, respectively. This phenomenon can be explained as follows: the Al powder almost did not lose their weight during the heating period, but experienced weight expansion through reacting with the heating atmosphere (N_2), gaseous byproducts generated during the polymer-to-ceramic conversation, or with the ceramic residue. Besides, with the increase on the percentages of Al filler in the matrix, the content of PSN1 with a large mass loss during the ceramization processes decreased.

3.2. Curing behaviors of PSN1 and PSN1/Al

The FT-IR analysis was used to assess the curing behavior of PSN1 with and without Al powder (Fig. 2). All samples were cured at 170 °C for 2 h under air atmosphere, and further treated at 450 °C for 1 h in nitrogen. PSN1 was cured by radical polymerization reaction of vinyl groups initiated by DCP [32]. The curing degree of PSN1 can be determined by the change of C3H stretching vibration in Si3CHåCH$_2$ around 3044 cm^{-1} [33]. According to the FT-IR spectra, after being treated at 170 °C for 2 h under air atmosphere, a weak absorption attributed to the C3H bonds was still shown in the spectra of PSN1 and PSN1/Al, which indicated that PSN1 was not completely cross-linked. Further thermal treatment at 450 °C for 1 h in nitrogen produced a well-cured sample, and C3H stretching vibration in Si3CHåCH$_2$ completely disappeared.

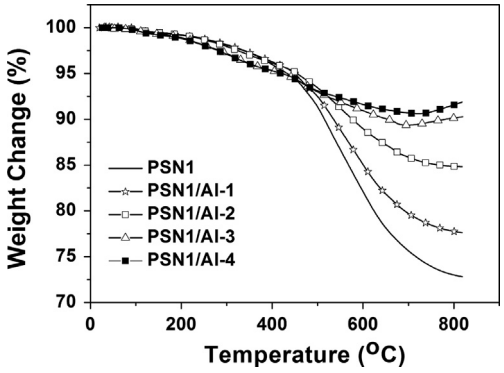

Fig. 1. TGA analyses of cross-linked PSN1 and PSN1/Al powders in nitrogen atmosphere.

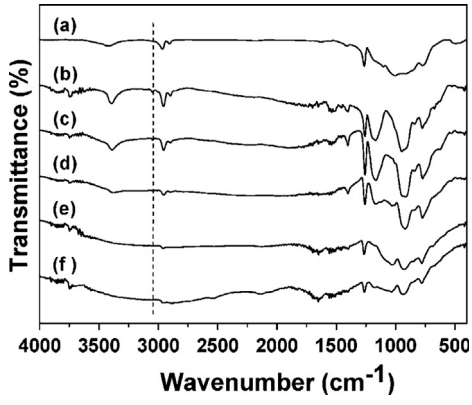

Fig. 2. FT-IR spectra of cross-linked PSN1 and PSN1/Al powders in the range of 4000–400 cm^{-1}: (a) PSN1-450 °C; (b) PSN1-170 °C; (c) PSN1/Al-1-170 °C; (d) PSN1/Al-2-170 °C; (e) PSN1/Al-3-170 °C; and (f) PSN1/Al-4-170 °C.

3.3. Chemical compositions of pyrolyzed PSN1 and PSN1/Al

The XRD diffraction patterns of PSN1 and PSN1/Al pyrolyzed at 800 °C in nitrogen atmosphere are shown in Fig. 3. It can be seen that the pyrolytic product of PSN1 powders obtained at 800 °C is fully amorphous. For the samples with different Al contents pyrolyzed at 800 °C, crystalline phases of Si, Al_2OC, and AlN were observed in their residues, and the peak belonging to Al disappeared. This indicated that all the Al powder completely reacted with the SiOCN matrix to form Al_2OC and AlN phases during the ceramization process, accompanied by volume expansion, where the oxygen in SiOCN ceramic derived from PSN1 was introduced during the curing process in air atmosphere. What's more, the diffraction intensities of crystal phases become more obvious with the increase of Al content, demonstrating that crystallization degree of the ceramic coatings increases. The presence of crystalline Si, suggested by the characteristic peaks at about 28.4°, 47.2°, 56.04°, and 76.4°, was also reported in earlier studies on polysiloxane/Al-derived ceramics, in which liquid Al could react with SiOC matrix as reaction (1) [34]. Similarly, a reaction between liquid Al and SiOCN matrix in N_2 atmosphere may occur following reaction (2). The presence of AlN may also result from reaction (2), and may also be attributed to reaction of the active filler Al with the nitrogen atmosphere, as reaction (3) [35].

$$3SiOC + 6Al \rightarrow Al_2O_3 + Al_4C_3 + 3Si \quad (1)$$

$$SiOCN + 3Al(l) \rightarrow Al_2OC + Si + AlN \quad (2)$$

$$2Al(S) + N_2 \rightarrow 2AlN \quad (3)$$

The XPS analysis was performed to further identify the formation of crystalline Si in the PSN1/Al samples pyrolyzed at 800 °C in nitrogen. As shown in Fig. 4, the peak of Si 2p for PSN1/Al-1, PSN1/Al-2, PSN1/Al-3, and PSN1/Al-4 pyrolyzed at 800 °C can be deconvoluted to four components: the peak centered at 99.2 eV is assigned to crystalline Si; the second around 101.4 eV is assigned to Si3N bonds or SiO_2C_2; the third at 103.5 eV is assigned to Si3O bonds; and the peak at an intermediate energy of 102.5 eV is attributed to silicon atoms bound to both nitrogen and oxygen [36–39]. Table 2 summarizes

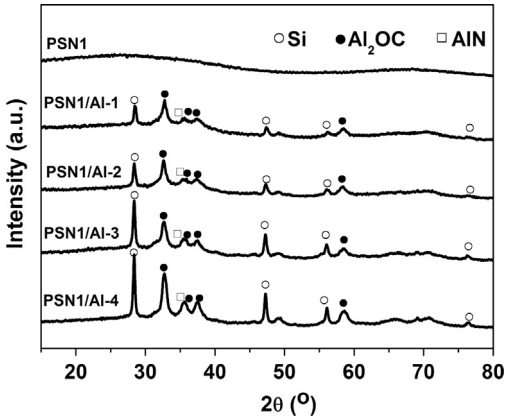

Fig. 3. X-ray diffraction patterns of PSN1 and PSN1/Al powders pyrolyzed at 800 °C in nitrogen.

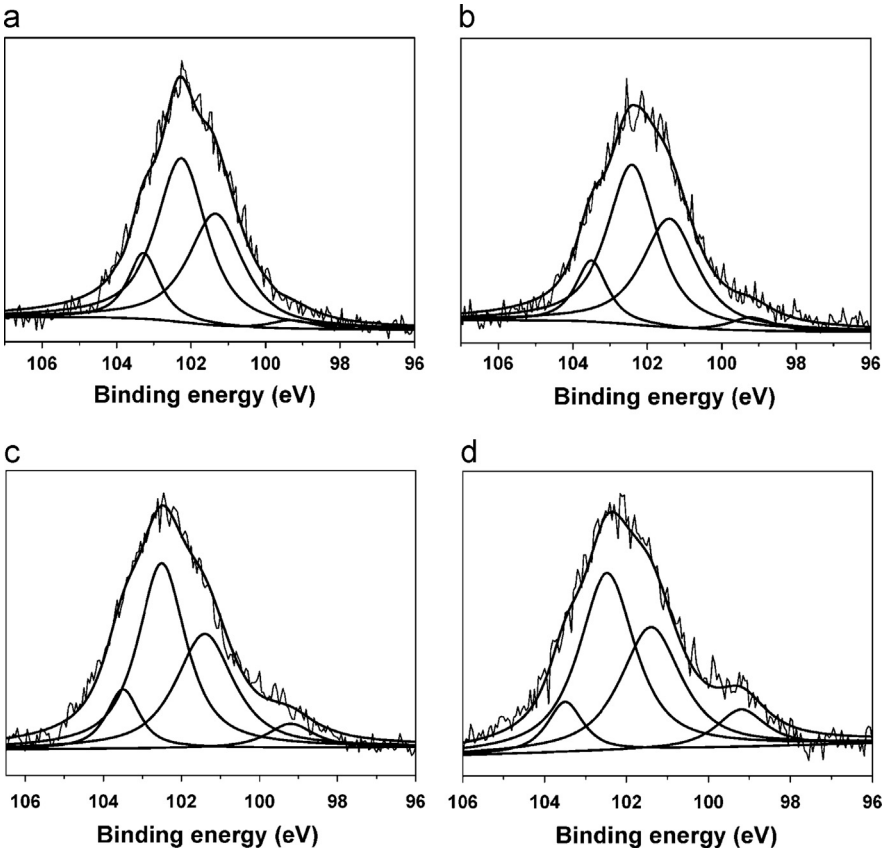

Fig. 4. XPS spectra of Si 2p for PSN1/Al pyrolyzed at 800 °C: (a) PSN1/Al-1; (b) PSN1/Al-2; (c) PSN1/Al-3; and (d) PSN1/Al-4.

the details concerning the deconvolution of XPS peaks, which are calculated from the experimental data in Fig. 4. All samples have their Si3O, Si3O3N, Si3N/SiO_2C_2, and Si binding energy (E_b) around 103.5, 102.4, 101.4, 99.2 eV, and full-width of half-maximum (FWHM) around 1.02, 1.60, 1.76, 1.43, indicating that the change of Al content does not affect the chemical bonding situation of the ceramic coatings. However, the ratio of the same ingredient in each sample was different. With the increase of Al addition, an increase in the crystalline Si content and a decrease in the other ingredients of the ceramic coatings were observed. According to reaction (2), with increase in the volume percent of Al filler, more SiOCN ceramics take part in crystallization reaction with Al. That is, with the increase of expansion agent Al, the contents of Si3N/SiO_2C_2, Si3O, and Si3O3N consumed as reactants, which comprise SiOCN ceramics, decrease and crystalline Si produced through the reaction increases.

3.4. Surface and cross section morphologies of the coatings

The surface morphologies of the ceramic coatings derived from PSN1 and PSN1/Al pyrolyzed at 800 °C for 1 h are presented in Fig. 5. It can be seen that some honeycomb cracks exist on the surface of the coating fabricated from pure PSN1 (Fig. 5(a)). The large weight loss during the pyrolysis of PSN1 as indicated in the TGA analyses is believed to account for the formation of the cracks [4]. In contrast, as shown in Fig. 5(b)–(e), the ceramic coatings prepared from PSN1/Al-1, PSN1/Al-2, PSN1/Al-3, and PSN1/Al-4 show uniform surface without crack, and the Al powder is distributed homogeneously in the ceramic matrix. Further inspection of the insets in Fig. 5(b)–(e) reveals that the

Table 2
The details concerning the deconvolution of XPS peaks.

Samples	Si3O	Si3O3N	Si3N/SiO_2C_2	Si
PSN1/Al-1				
E_b (eV)	103.3	102.3	101.3	99.3
FWHM	1.02	1.6	1.75	1.43
r_i[a] (%)	12.5	48.7	36.4	2.41
PSN1/Al-2				
E_b (eV)	103.5	102.4	101.4	99.2
FWHM	1.02	1.6	1.76	1.43
r_i (%)	11.8	48.3	36.2	3.62
PSN1/Al-3				
E_b (eV)	103.5	102.5	101.4	99.2
FWHM	1	1.59	1.76	1.43
r_i (%)	10.5	48	35.4	6.08
PSN1/Al-4				
E_b (eV)	103.5	102.5	101.4	99.2
FWHM	1.03	1.62	1.76	1.43
r_i (%)	8.53	47.3	35.3	8.81

[a]The ratio $A_i/\sum A_i$ (A_i is the area of each deconvoluted peak).

surface of ceramic coatings with less Al content is more dense and continuous, while the surface of those with more content of Al powder becomes loose and rough. With increase in the volume percent of Al filler, more SiOCN ceramics were involved in crystallization reaction with Al, which resulted in a break in the continuity of the microstructures and produced looser coatings.

The cross section morphologies of the coatings are shown in Fig. 6. The thickness for the coatings derived from PSN1/Al-1, PSN1/Al-2, PSN1/Al-3, and PSN1/Al-4 is about 1.5 μm, 2.1 μm, 2.9 μm, and 5.5 μm, respectively. It is clear that the coatings become thicker with increase of the volume percent of Al expansion agent, which is attributed to the enhancement of the ceramic yield and the increase of slurry viscosity from PSN1/Al-1 to PSN1/Al-4, as shown in the TGA analysis (Fig. 1), and Table 1, respectively. No through-thickness cracks and pores can be detected in the whole cross section of the composite coatings. Furthermore, there is no delamination at the interface of the coatings prepared from PSN1/Al-1, PSN1/Al-2, and PSN1/Al-3, indicating strong adhesion between coating and steel substrate. However, for the coating derived from PSN1/Al-4, partially peeling off of the composite coating from the substrate took place. The delamination may be from the cutting and polishing process during sample preparation, but it suggests the weak adhesion between the coating and substrate, which arises from the mismatch of coefficient of thermal expansion between the steel and crystalline phase. With the increase of Al content, the crystallization degree of coating becomes more obvious, which aggravates the thermal mismatch, and hence results in the delamination. On the basis of surface and cross section morphologies analyses, it is reasonable to assert that the introduction of 10–40 vol% of Al expansion agent could effectively avoid the formation of cracks and unwanted porosity. However, when the volume fraction of Al exceeds 30%, the obtained coatings tend to exfoliate. Therefore, the optimum range of Al content is 10–30 vol%.

3.5. Mechanical properties of the coatings

The surface hardness and elastic modulus of PSN1/Al-based coatings on 304 steel were investigated by nano-indentation (Fig. 7). The data were determined by the average value of 5 measurements with a contact depth ranging from 50 to 300 nm. The surface hardness and elastic modulus of coating are easily affected by the surface hardness of substrate when the displacement depth is larger than 20% of the thickness of the coating [40]. The thickness of the thinnest ceramic coating in this study is about 1.5 μm. The largest displacement depth,

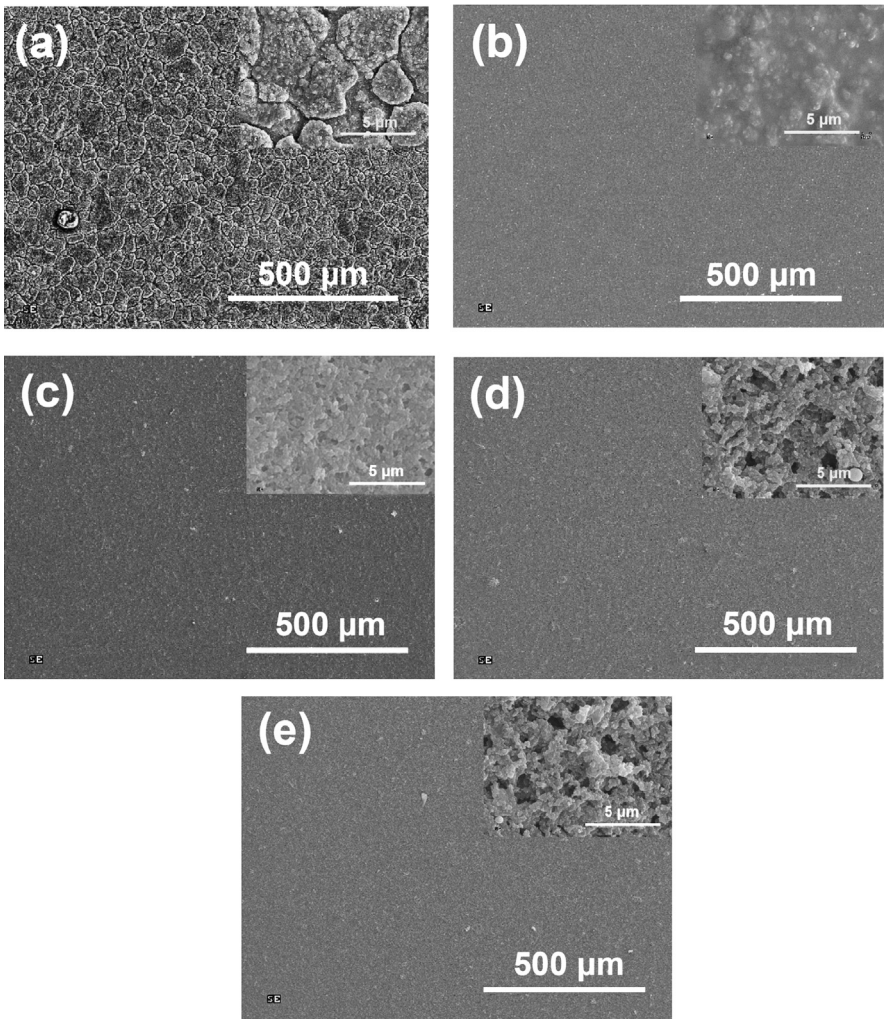

Fig. 5. Surface morphologies of PSN1 and PSN1/Al-based coatings on 304 steel: (a) PSN1; (b) PSN1/Al-1; (c) PSN1/Al-2; (d) PSN1/Al-3; and (e) PSN1/Al-4.

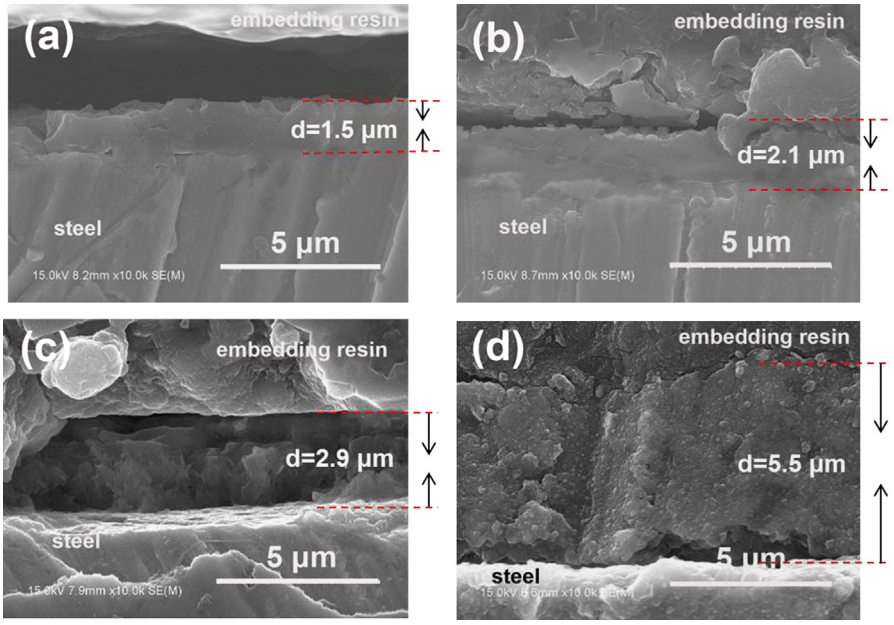

Fig. 6. Cross section morphologies of PSN1/Al-based coatings on 304 steel: (a) PSN1/Al-1; (b) PSN1/Al-2; (c) PSN1/Al-3; and (d) PSN1/Al-4.

300 nm, used in our work, corresponds to approximately 20% of the coating thickness, therefore the substrate-effect can be negligible.

Fig. 7(a) displays the surface hardness of the ceramic coatings as a function of the volume percent of Al expansion agent. With the increase of Al addition, an obvious decrease in the surface hardness of the ceramic coatings was observed. The surface hardness of the ceramic coatings derived from PSN1/Al-1 is about 6.38 GPa. While, the hardness of the coatings based on PSN1/Al-4 falls to 1.63 GPa. According to the microstructure shown in Fig. 5, the increase of expansion agent Al leads to a looser structure of the coating, which further results in a decrease of the hardness [41].

Fig. 7(b) shows the relationship between the elastic modulus of PSN1/Al-based coatings and Al expansion agent content. It can be seen that the Al expansion agent content has the same effect on the elastic modulus as on the surface hardness of the ceramic coatings. The elastic modulus decreases with increase in the volume percent of Al filler. Also, this is due to the reduced densification with increase of Al content.

4. Conclusions

We successfully fabricated ceramic coatings with the thickness range of 1.5–5.5 μm on 304 stainless steel substrate using polysilazane (PSN1) as a preceramic polymer and Al powder as an active filler. The volume of Al powder in the matrix had a significant effect on the crystallization degree and microstructure of the ceramic coatings, thereby greatly affecting their mechanical properties. With the increase of Al content, the crystallization degree of coating became more obvious. Furthermore, when Al content was in the range of 10–40% (Al/PSN1, v/v), the surface of ceramic coating was uniform and crackless, whereas the Al content was not more than 30 vol% in consideration of adhesion between the coating and substrate. Surface hardness of the ceramic coatings drastically

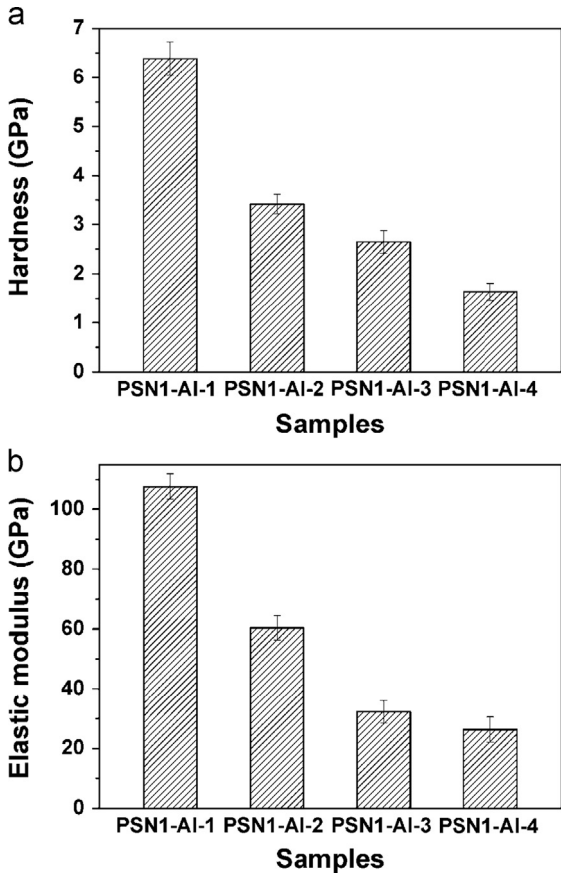

Fig. 7. The surface hardness and elastic modulus of PSN1/Al-based coatings on steel 304: (a) hardness and (b) elastic modulus.

decreased from 6.38 to 1.63 GPa, and elastic modulus of the coatings decreased from 107.66 to 26.32 GPa with increasing the volume fraction of Al from 10% to 40%. Further work will be done on the investigation of the environmental barrier properties of the ceramic coatings under extreme conditions such as in combustion environments.

Acknowledgments

The authors thank the National Science Foundation of China (NSFC, No. 50973113) for financial support.

References

[1] P. Colombo, G. Mera, R. Riedel, G.D. Sorarù, Polymer-derived ceramics: 40 years of research and innovation in advanced ceramics, Journal of the American Ceramic Society 93 (2010) 1805–1837.
[2] M. Günthner, T. Kraus, A. Dierdorf, D. Decker, W. Krenkel, G. Motz, Advanced coatings on the basis of Si (C) N precursors for protection of steel against oxidation, Journal of the European Ceramic Society 29 (2009) 2061–2068.
[3] M. Günthner, A. Schütz, U. Glatzel, K. Wang, R.K. Bordia, O. Greißl, W. Krenkel, G. Motz, High performance environmental barrier coatings, Part I: passive filler loaded SiCN system for steel, Journal of the European Ceramic Society 31 (2011) 3003–3010.
[4] J.D. Torrey, R.K. Bordia, C.H. Henager, Y. Blum, Y. Shin, W. D. Samuels, Composite polymer derived ceramic system for oxidizing environments, Journal of Materials Science 41 (2006) 4617–4622.
[5] O. Funayama, T. Kato, Y. Tashiro, T. Isoda, Synthesis of a polyborosilazane and its convertion into inorganic compounds, Journal of the American Ceramic Society 76 (1993) 717–723.
[6] S.R. Shah, R. Raj, Mechanical properties of a fully dense polymer derived ceramic made by a novel pressure casting process, Acta Materialia 50 (2002) 4093–4103.
[7] S. Martinez-Crespiera, E. Ionescu, H.J. Kleebe, R. Riedel, Pressureless synthesis of fully dense and crack-free SiOC bulk ceramics via photocrosslinking and pyrolysis of a polysiloxane, Journal of the European Ceramic Society 31 (2011) 913–919.
[8] T. Xu, Q. Ma, Z. Chen, High-temperature behavior of Cf/SiOC composites in inert atmosphere, Materials Science and Engineering A 530 (2011) 266–270.
[9] Q. Li, S. Dong, Z. Wang, G. Shi, Fabrication and properties of 3-D Cf/$ZrB_2$3ZrC3SiC composites via polymer infiltration and pyrolysis, Ceramics International 39 (2012) 5937–5941.
[10] S. Bernard, M. Weinmann, D. Cornu, P. Miele, F. Aldinger, Preparation of high-temperature stable SiBCN fibers from tailored single source polyborosilazanes, Journal of the European Ceramic Society 25 (2005) 251–256.
[11] L. Gottardo, S. Bernard, C. Gervais, K. Inzenhofer, G. Motz, M. Weinmann, C. Balan, P. Miele, Chemistry, structure and processability of boron-modified polysilazanes as tailored precursors of ceramic fibers, Journal of Materials Chemistry 22 (2012) 7739–7750.
[12] E. Bernardo, G. Parcianello, P. Colombo, J. Adair, A. Barnes, J. Hellmann, B. Jones, J. Kruise, J. Swab, SiAlON ceramics from preceramic polymers and nano-sized fillers: application in ceramic joining, Journal of the European Ceramic Society 32 (2012) 1329–1335.
[13] H. Schmidt, D. Koch, G. Grathwohl, P. Colombo, Micro-/macroporous ceramics from preceramic precursors, Journal of the American Ceramic Society 84 (2001) 2252–2255.
[14] C. Vakifahmetoglu, I. Menapace, A. Hirsch, L. Biasetto, R. Hauser, R. Riedel, P. Colombo, Highly porous macro- and micro-cellular ceramics from a polysilazane precursor, Ceramics International 35 (2009) 3281–3290.
[15] J. Wu, Y. Li, L. Chen, Z. Zhang, D. Wang, C. Xu, Simple fabrication of micro/nano-porous SiOC foam from polysiloxane, Journal of Materials Chemistry 22 (2012) 6542–6545.
[16] L.-A. Liew, W. Zhang, V.M. Bright, L. An, M.L. Dunn, R. Raj, Fabrication of SiCN ceramic MEMS using injectable polymer-precursor technique, Sensors and Actuators A 89 (2001) 64–70.
[17] L.-A. Liew, Y. Liu, R. Luo, T. Cross, L. An, V.M. Bright, M.L. Dunn, J. W. Daily, R. Raj, Fabrication of SiCN MEMS by photopolymerization of pre-ceramic polymer, Sensors and Actuators A 95 (2002) 120–134.
[18] J. Liu, L. Zhang, J. Yang, L. Cheng, Y. Wang, Fabrication of SiCN–$Sc_2Si_2O_7$ coatings on C/SiC composites at low temperatures, Journal of the European Ceramic Society 32 (2012) 705–710.
[19] L. Hu, M. Li, C. Xu, Y. Luo, Y. Zhou, A polysilazane coating protecting polyimide from atomic oxygen and vacuum ultraviolet radiation erosion, Surface and Coatings Technology 203 (2009) 3338–3343.
[20] B. Gardelle, S. Duquesne, C. Vu, S. Bourbigot, Thermal degradation and fire performance of polysilazane-based coatings, Thermochimica Acta 519 (2011) 28–37.
[21] M. Monti, B. Dal Bianco, R. Bertoncello, S. Voltolina, New protective coatings for ancient glass: silica thin-films from perhydropolysilazane, Journal of Cultural Heritage 9 (2008) e143–e145.
[22] T.J. Cross, R. Raj, S.V. Prasad, D.R. Tallant, Synthesis and tribological behavior of silicon oxycarbonitride thin films derived from poly(urea) methyl vinyl silazane, International Journal of Applied Ceramic Technology 3 (2006) 113–126.
[23] A. Morlier, S. Cros, J.-P. Garandet, N. Alberola, Thin gas-barrier silica layers from perhydropolysilazane obtained through low temperature curings: a comparative study, Thin Solid Films 524 (2012) 62–66.
[24] A. Asthana, Y. Asthana, I.K. Sung, D.P. Kim, Novel transparent poly (silazane) derived solvent-resistant, bio-compatible microchannels and substrates: application in microsystem technology, Lab on a Chip 6 (2006) 1200–1204.
[25] B. Hoffmann, M. Feldmann, G. Ziegler, Sol–gel and precursor-derived coatings with cover function on medical alloys, Journal of Materials Chemistry 17 (2007) 4034–4040.
[26] M. Scheffler, P. Greil, A. Berger, E. Pippel, J. Woltersdorf, Nickel-catalyzed in situ formation of carbon nanotubes and turbostratic carbon in polymer-derived ceramics, Materials Chemistry and Physics 84 (2004) 131–139.
[27] J.D. Torrey, R.K. Bordia, Processing of polymer-derived ceramic composite coatings on steel, Journal of the American Ceramic Society 91 (2008) 41–45.
[28] P. Colombo, E. Bernardo, G. Parcianello, Multifunctional advanced ceramics from preceramic polymers and nano-sized active fillers, Journal of the European Ceramic Society 33 (2013) 453–469.
[29] K. Wang, M. Günthner, G. Motz, R.K. Bordia, High performance environmental barrier coatings, Part II: active filler loaded SiOC system for superalloys, Journal of the European Ceramic Society 31 (2011) 3011–3020.
[30] Y.M. Wang, H. Tian, D.L. Quan, L.X. Guo, J.H. Ouyang, Y. Zhou, D. C. Jia, Preparation, characterization and infrared emissivity properties of polymer derived coating formed on 304 steel, Surface and Coatings Technology 206 (2012) 3772–3776.
[31] D. Yang, Y. Yu, X. Zhao, Y. Song, E. Lopez-Honorato, P. Xiao, D. Lai, Fabrication of silicon carbide (SiC) coatings from pyrolysis of polycarbosilane/aluminum, Journal of Inorganic and Organometallic Polymers 21 (2011) 534–540.
[32] Z. Zhang, W. Shen, C. Ye, Y. Luo, S. Li, M. Li, C. Xu, Y. Song, Large-area, crack-free polysilazane-based photonic crystals, Journal of Materials Chemistry 22 (2012) 5300–5303.
[33] M. Günthner, K. Wang, R.K. Bordia, G. Motz, Conversion behaviour and resulting mechanical properties of polysilazane-based coatings, Journal of the European Ceramic Society 32 (2012) 1883–1892.
[34] L. Toma, C. Fasel, S. Lauterbach, H.J. Kleebe, R. Riedel, Influence of nano-aluminum filler on the microstructure of SiOC ceramics, Journal of the European Ceramic Society 31 (2011) 1779–1789.
[35] Z. Xie, S. Wang, Z. Chen, Active filler (aluminum–aluminum nitride) controlled polycarbosilane pyrolysis, Journal of Inorganic and Organometallic Polymers 16 (2006) 69–81.
[36] W. Liu, M. Zhang, C. Lin, Z. Zeng, L. Wang, P.K. Chu, Intense blue-light emission from carbon-plasma-implanted porous silicon, Applied Physics Letters 78 (2001) 37–39.

[37] L. Hu, M. Li, C. Xu, Y. Luo, Perhydropolysilazane derived silica coating protecting Kapton from atomic oxygen attack, Thin Solid Films 520 (2011) 1063–1068.
[38] O. Funayama, H. Nakahara, M. Okoda, M. Okumura, T. Isoda, Conversion mechanism of polyborosilazane into silicon nitride-based ceramics, Journal of Materials Science 30 (1995) 410–416.
[39] Y. Yu, H. Jung, J. Lee, S. Hwang, Y. Kim, H. Kim, Silicon dioxide thin film derived from polyphenylcarbosilane under an oxidizing atmosphere, Thin Solid Films 519 (2011) 5706–5711.
[40] R. Saito, S. Kobayashi, H. Hayashi, T. Shimo, Surface hardness and transparency of poly(methyl methacrylate)-silica coat film derived from perhydropolysilazane, Journal of Applied Polymer Science 104 (2007) 3388–3395.
[41] R. Wang, W. Pan, J. Chen, M. Jiang, Y. Luo, M. Fang, Properties and microstructure of machinable Al_2O_3/$LaPO_4$ ceramic composites, Ceramics International 29 (2003) 19–25.